EURASIAN PHYSICAL TECHNICAL JOURNAL

2024, Volume 21, No.3 (49)

https://doi.org/10.31489/2024No3/37-44

Received: 12/02/2024 Revised: 17/04/2024 Accepted: 14/08/2024 Published online: 30/09/2024

Original Research Article

UDC 537.9

DETERMINATION OF THE ELEMENTAL COMPOSITION AND CHANGES IN THERMAL AND ELECTRICAL CONDUCTIVITY OF "HANFORD" AND LOW-ASH MEDIUM-GRAINED GRAPHITE'S GRADE GRAPHITES DEPENDING ON THE FAST NEUTRONS FLUENCE

Baytelesov S.A., Tojiboev D.D., Sadikov I.I., Kungurov F.R., Alikulov Sh.A.

Institute of Nuclear Physics of Uzbekistan Academy of Sciences, Tashkent, Uzbekistan
*Corresponding author: baytel@inp.uz

Abstract. *Studying the properties of graphite recovered from operating nuclear reactors is vital for predicting the properties and integrity of graphite as part of assessing the continued operation and life extension of nuclear reactors. The purpose of the study is to determine the electrical conductivity and thermal conductivity of low-ash medium-grained graphite's grade graphite in the thermal column masonry of the VVR-SM research reactor in the measurement temperature range corresponding to the conditions of normal operation of the reactor to determine the service life. In this work, the change in thermal conductivity and electrical conductivity of GMZ graphite was studied, as well as for comparison of Hanford grade graphite depending on the fluence of fast neutrons and the measurement temperature. The dependence of electrical conductivity and thermal conductivity on dose and temperature has been established. It has been shown that the greater the neutron fluence, the more both the thermal conductivity and electrical conductivity of the material decreases. The service life of the thermal column has been determined.*

Keywords: thermal conductivity, electrical conductivity, low-ash medium-grained graphite's, "Hanford" grade graphite, fast neutrons, fluence, dose.

1. Introduction

The development of nuclear technology is moving in the direction of increasing energy and heat intensity, the intensity of radiation exposure on individual structural elements of nuclear reactors, which puts forward increased demands on the materials used. Especially for high-temperature gas-cooled reactors (HTGR) and thermonuclear reactors (TNR). Among others, carbon-graphite materials are increasingly used in nuclear technology, not only as a masonry material, but also for structural elements. For example, for claddings and matrices of spherical fuel elements, coatings of microfuel elements in HTGR, screens in nuclear reactors, etc. Naturally, depending on the operating conditions (neutron fluence, irradiation intensity and temperature), the requirements for materials for these installations differ significantly from the usual requirements for nuclear graphite [1].

The works [2-7] investigated the properties of graphite materials for a high-temperature gas-cooled reactor, such as the electronic structure and properties of composites based on the carbon isotope, the durability of reactor graphites, and the thermal conductivity of graphite. Natural carbon has two stable isotopes - ^{12}C (98.892%) and ^{13}C (1.108%). There are also four radioactive isotopes (^{10}C, ^{11}C, ^{14}C and ^{15}C), of which only the ^{14}C isotope is long-lived with a half-life of 5730 years. The neutron absorption cross sections in the reaction with carbon nuclei are less than 4.5 microbarns for high-purity graphite [8]. Most of the collisions of neutrons with carbon nuclei in this case occur via the elastic scattering mechanism. The latter circumstance determined

the effective use of graphite as a moderator. In particular, for a nuclear reactor operating on enriched uranium, graphite, as a moderator, is second in efficiency to beryllium and heavy water. In this case, high-purity graphite is used, where the total impurity content does not exceed 1×10^{-3}%.

Graphite serves as a key material for heat dissipation in electronic devices and nuclear engineering due to its remarkable thermal properties [1]. Thermal expansion and conductivity of graphite have always been the main scientific parameters in the field of carbon materials. Therefore, great attention is paid to theoretical and experimental research in this area. It is known that neutron irradiation noticeably reduces the electrical and thermal conductivity of graphite materials [9]. When nuclear graphite is annealed, Wigner energy is released [10]. The thermal conductivity values of individual grades of graphite vary greatly from each other, this is the result of different production processes leading to differences in the microstructure of the final product [11].

Studying the properties of graphite recovered from operating nuclear reactors is vital for predicting the properties and integrity of graphite as part of assessing continued operation and life extension of a nuclear plant [12]. Reactors have limited space available for monitoring structural materials, so size-constrained samples require reliable and efficient measurement methods.

2. Materials and experimental methods

Graphite samples taken from the "residual" graphite stockpile from the construction of the B reactor in the 1940s (the first graphite reactor at the Hanford site) were prepared and represent first-generation nuclear reactor graphite. Samples of "Hanford" grade graphite, representing a cylinder with a diameter d=Ø12 mm and a height h=19 mm, weighing 4.79 g, from which samples for irradiation with a diameter d=Ø12 mm and a height h=3.4 mm, weighing 0.6 g were prepared.

Samples of GMZ (low-ash medium-grained graphite's) grade graphite with a diameter d=Ø16 mm and a height h=3.64 mm, weighing 1.3 g, as well as a prism type, a=8.18 mm, b=7.95 mm, L=59.1 mm, m=6.3 g were prepared. GMZ grade graphite is characterized by high density (>1.8 kg/m^3) and electrical conductivity, low porosity (7%) and gas permeability. It is heat- and wear-resistant, chemically inert. Graphite hardness – 52 Shore, ash content <0.1%, grain size <10 microns.

The samples were placed in the vertical channels of the VVR-SM research reactor of the Institute of Nuclear Physics of Academy of Sciences, Republic of Uzbekistan (INP AS RU) with a modified loading scheme at 10 MW power for irradiation with fast neutrons. Vertical channels 1-5 and 1-3 were used in the reactor core, where the fast neutron flux density (E_n>0.8 MeV) in the channels was 1.19×10^{13} n/(cm$^2\times$s) and 9.72×10^{12} n/(cm$^2\times$s), respectively.

The temperature in the channel was maintained at about 318 K. The heat released due to radiation heating was removed by circulating primary circuit water at a volumetric rate of 1250 m^3/hour. Measurements of the thermal conductivity coefficient in the original samples and those irradiated with various doses were carried out using the dynamic calorimeter method on an IT-λ-400 installation in the temperature range from 290 K to 490 K.

The value of the thermal conductivity coefficient was calculated from the results of measuring the thickness, cross-sectional area of disk samples and the temperature difference in the sample and the heat meter, using the relationship [13,14]:

$$\lambda = K_T \cdot \frac{n_t}{n_0} \cdot \frac{h}{S(1+\sigma_C)} \quad , \tag{1}$$

where n_t and n_0 are, respectively, the temperature differential in the heat-meter rod and the sample, respectively; h and S are, respectively, the height and area of the transverse cross section of the sample; K_T is the thermal conductivity of the heat-meter rod; and σ_C is the correction for the specific heat of the sample.

A chemically pure copper sample was used as a thermal conductivity standard when determining the thermal conductivity of the heat meter K_T. The above formula did not take into account the influence of the specific contact thermal resistance P_k, the relative contribution of which to the total thermal resistance of the sample and the heat meter rod is negligibly small. The thermal conductivity coefficient was determined with an error of no more than 10%.

The electrical resistance of graphite samples was measured using a four-probe compensation method at a current of 1 mA [15,16] in the temperature range from 290 K to 490 K. Electrical resistivity ρ was determined from the relation:

$$\rho = \frac{U \cdot S \cdot R_{et}}{L \cdot U_{et}} \tag{2}$$

where U and U_{et} are the voltage drop across the measured and reference samples, R_{et} is the resistance of the reference coil, equal to 0.01 Ohm, S and L are the cross section and length of the sample, respectively. Electrical conductivity coefficients were determined with an error of no more than 10%.

3. Results of experiments and calculations

Solid (piece) and powder of the GMZ grade graphite were prepared to determine the impurity composition of the sample. Figure 1 shows an electronic image of the GMZ grade graphite surface and its elemental composition using an EVO MA10 scanning electron microscope.

Table 1 shows the percentage of impurities of GMZ grade graphite obtained using an EVO MA10 scanning electron microscope.

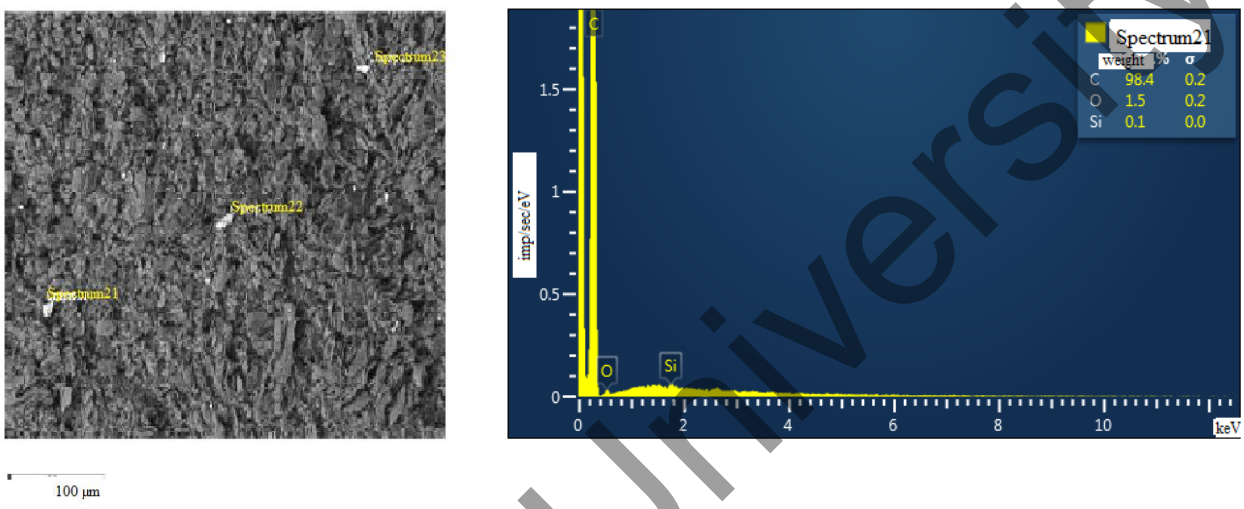

a) graphite surface image b) elemental composition of GMZ grade graphite

Fig. 1. Electronic image of the GMZ grade graphite surface and elemental composition.

Table 1. Content of impurities of GMZ grade graphite

Element	Type of line	Conditional concentration	Weight, %	Accuracy Weight, %	Standard name
C	K series	2.41	98.39	0.25	C Vit
O	K series	0.02	1.51	0.24	SiO_2
Si	K series	0.00	0.11	0.05	SiO_2
Sum:			100.00		

Figure 1 shows areas with different contrasts, which indicate the presence of impurity elements such as oxygen and silicon and others in the graphite matrix. To test the assumption, the content of impurity elements in the samples was determined using the technique of instrumental neutron activation analysis of elements. The content of impurity elements in the samples was determined.

To measure the samples, a gamma spectrometer with a GC-1820 semiconductor detector and an InSpector-2000 multichannel analyzer with Genie-2000 software (CANBERRA USA) was used. To calculate the concentration of impurity elements, IAEA standards with certified contents of elements in soil and bottom sediments were used. Table 2 shows the results of determining the content of impurity elements in the GMZ grade of graphite, obtained by instrumental neutron activation analysis.

Table 2. Content of impurity elements in GMZ grade graphite.

Element	Concentration, C ± ΔC, ppm (μg/g)	Concentration, C ± ΔC, ppm (μg/g))	Element	Concentration, C ± ΔC, ppm (μg/g)	Concentration, C ± ΔC, ppm (μg/g)
	Graphite piece	Graphite powder		Graphite piece	Graphite powder
As	(2.96 ± 0.09) E-02	(1.24 ± 0.07) E-01	Nd	(7.52 ± 0.83) E-01	(1.26 ± 0.23)
Ba	(7.48 ± 0.60)	(1.50 ± 0.27) E+01	Ni	(8.60 ± 1.03) E-01	(2.73 ± 0.63)
Br	(4.16 ± 0.40) E-02	(3.65 ± 0.13) E-01	Rb	(5.33 ± 0.69) E-02	(3.88 ± 0.39) E-01
Ce	(1.59 ± 0.13)	(2.33 ± 0.19)	Sb	(8.90 ± 0.71) E-03	(1.02 ± 0.09) E-01
Co	(1.79 ± 0.20) E-02	(1.69 ± 0.19) E-01	Sc	(2.83 ± 0.11) E-01	(4.12 ± 0.16) E-01
Cr	(8.28 ± 0.75) E-02	(5.40 ± 0.38)	Se	(3.96 ± 0.59) E-03	(2.10 ± 0.76) E-02
Cs	(8.25 ± 1.32) E-03	(2.25 ± 0.36) E-02	Sm	(7.53 ± 0.45) E-02	(1.48 ± 0.10) E-01
Eu	(1.42 ± 0.12) E-02	(2.01 ± 0.17) E-02	Sr	(3.10 ± 0.43)	(5.10 ± 0.72)
Fe	(5.30 ± 0.27) E-04	(4.51 ± 0.17) E-02	Ta	(2.14 ± 0.30) E-03	(5.76 ± 0.98) E-03
Hf	(8.23 ± 1.25) E-03	(2.35 ± 0.53) E-02	Tb	(2.60 ± 0.26) E-02	(4.03 ± 0.13) E-02
K	(9.69 ± 1.98)	(6.51 ± 1.33) E+01	Th	(2.92 ± 0.23) E-02	(5.55 ± 0.78) E-02
La	(7.79 ± 0.62) E-01	(1.23 ± 0.10)	U	(5.71 ± 0.79) E-02	(1.22 ± 0.11) E-01
Lu	(1.31 ± 0.09) E-02	(2.36 ± 0.33) E-02	W	(3.60 ± 0.40) E-02	(9.17 ± 0.73) E-01
Mn	(1.66 ± 0.22) E-01	(5.14 ± 0.41)	Yb	(7.92 ± 0.46) E-03	(1.78 ± 0.24) E-02
Mo	(1.56 ± 0.14) E-01	(4.18 ± 0.67) E-01	Zn	(5.79 ± 0.87) E-01	(1.02 ± 0.15) E+01
Na	(2.39 ± 0.25)	(3.19 ± 0.21) E+01			

Figure 2 shows electron images of the "Hanford" grade graphite surface and its elemental composition using an EVO MA10 scanning electron microscope.

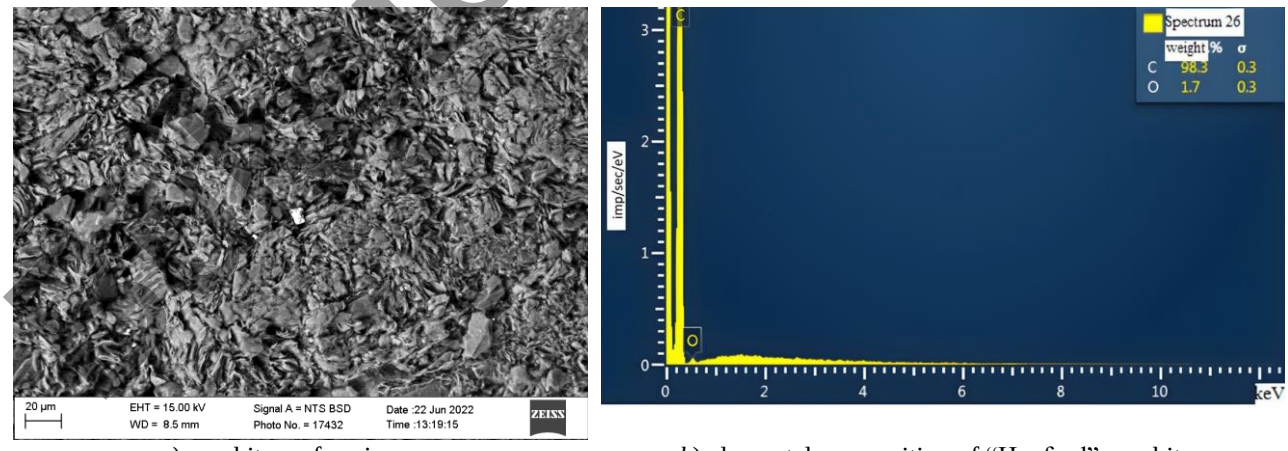

a) graphite surface image

b) elemental composition of "Hanford" graphite

Fig. 2. Electron image of the "Hanford" grade graphite surface and its elemental composition.

Table 3 shows the percentages of impurities in "Hanford" grade graphite obtained using an EVO MA10 scanning electron microscope.

Table 3. Impurity content in "Hanford" grade graphite.

Element	Type of line	Conditional concentration	Weight, %	Accuracy Weight, %	Standard name
C	K series	3.75	98.32	0.29	C Vit
O	K series	0.03	1.68	0.29	SiO_2
Sum:			100.00		

The content of impurity elements in the samples was determined using the technique of instrumental neutron activation analysis of elements. We used a CANBERRA semiconductor gamma spectrometer with Genie-2000 software, an AB204-S/FACT Mettler Toledo analytical balance, and a VM5101 VESTA laboratory balance to measure the samples. IAEA standards with certified contents of elements in soil and bottom sediments were also used. Table 4 shows the results of determining the content of impurity elements in the "Hanford" grade graphite.

Table 4. Content of impurity elements in the "Hanford" grade graphite (1 ppm = 1 μg/g)

"Hanford" grade graphite (KSO/CSO)		
Element	Concentration, ppm	
	Minimal	Maximal
Al	0.3	0.5
B	2.8	3
Ba	2.6	2.6
Ca	135	210
Cr	0.3	1.1
Cu	0.2	0.6
Fe	2.8	5.6
Li	0.2	0.3
Ni	0.3	2.5
S	31	33
Si	1.3	6
Sr	3.1	4
Ti	7.5	8.2
V	11	12
Zn	5.4	160

Table 5 shows the results of the electrical conductivity measurements of GMZ grade graphite, non-irradiated and irradiated with a neutron fluence of 1.59×10^{19} n/cm^2, depending on temperature.

Table 5. Electrical conductivity of GMZ grade graphite, non-irradiated and irradiated with a neutron fluence of 1.59×10^{19} n/cm^2, depending on temperature.

K	Non-irradiated ρ, Ohm×m	Irradiated ρ, Ohm×m
298	$11.4\cdot10^{-6}$	$31.7\cdot10^{-6}$
323	$11.2\cdot10^{-6}$	$31.5\cdot10^{-6}$
348	$11\cdot10^{-6}$	$31.3\cdot10^{-6}$
373	$10.8\cdot10^{-6}$	$31\cdot10^{-6}$
398	$10.7\cdot10^{-6}$	$30.6\cdot10^{-6}$
423	$10.5\cdot10^{-6}$	$30.1\cdot10^{-6}$
448	$10.3\cdot10^{-6}$	$29.7\cdot10^{-6}$

Figures 3 and 4 show the results of the thermal conductivity measurements of GMZ and "Hanford" grade graphite's irradiated with a fluence of 3.17×10^{19} n/cm^2, depending on the sample temperature. The temperature

dependence of the graphite thermal conductivity should be determined by the dependence of carrier mobility on temperature. The periodicity of the crystal lattice potential in the samples, disrupted by thermal vibrations, is additionally disrupted by randomly distributed impurity atoms. This leads to additional scattering of charge carriers and a decrease in their mobility. As a result, the thermal conductivity of graphite, depending on the neutron fluence, decreases. As can be seen from Figure 3, at a temperature of 298 K, the thermal conductivity of GMZ grade graphite with a 3.17×10^{19} n/cm^2 neutron fluence decreases by about 22% relative to the non-irradiated sample.

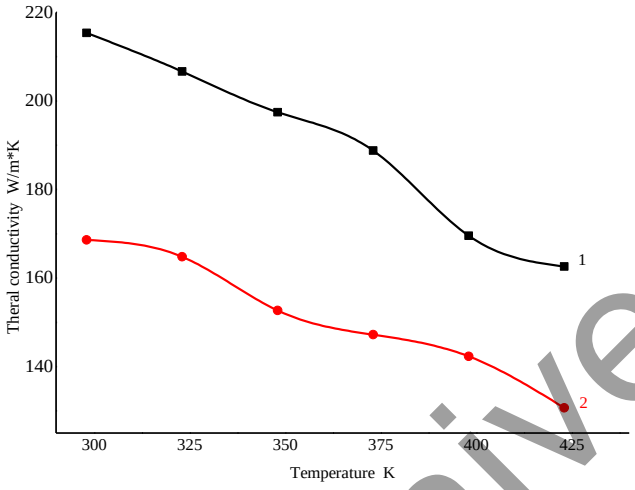

Fig.3. Thermal conductivity λ(T) of GMZ grade graphite samples before and after irradiation with 3.17×10^{19} n/cm^2 neutrons fluence, depending on the sample temperature. 1 – non-irradiated sample; 2 - irradiated sample.

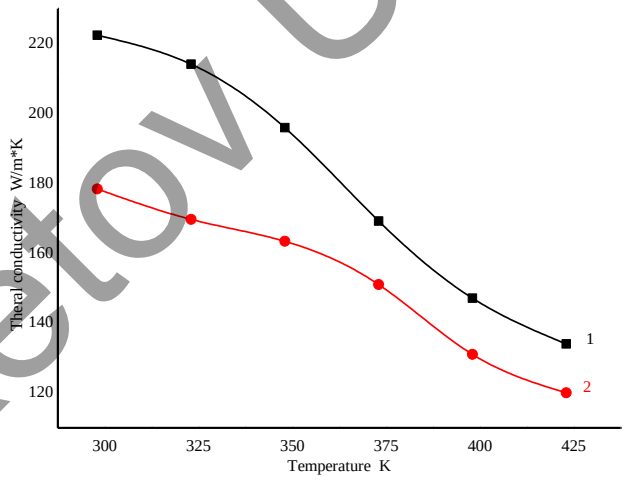

Fig. 4. Dependence of thermal conductivity λ(T) of "Hanford" grade graphite samples before and after irradiation with 3.19×10^{19} n/cm^2 neutrons fluence, depending on the sample temperature. 1 – Non-irradiated sample; 2 - irradiated sample.

Figure 4 shows that the thermal conductivity of "Hanford" grade graphite at a temperature of 298 K with a 3.17×10^{19} n/cm^2 neutron fluence decreases by about 20%, relative to the non-irradiated sample. In this case, a decrease in thermal conductivity was observed depending on the temperature of the sample in the range from 298 K to 423 K. The resistivity value of GMZ grade graphite at room temperature before irradiation was 1.14×10^{-7} Ohm×m. The resistivity value of GMZ grade graphite as a result of irradiation increased by 2.78 times and amounted to 3.17×10^{-7} Ohm×m. The increase in resistivity is due to the formation of defects as a result of irradiation of samples with fast neutrons in the VVR-SM reactor core.

In this case, a decrease in resistivity was observed depending on the increase in sample temperature in the range from 298 K to 423 K. This is due to an increase in the mobility of charge carriers with increasing

temperature. An increase in resistivity, as well as a decrease in thermal conductivity of G347A graphite at high fluence, was also noted in the work [17].

4. Conclusion

Thus, the analysis of the obtained experimental results made it possible to establish that the electrical and thermal conductivity of graphite varies with both temperature and irradiation dose. In this case, with increasing neutron fluence, the deviation from the linear dependence and, accordingly, the rate of decrease in the electrical and thermal conductivity of graphite decreases with temperature. It is known that at low fluences ($<10^{18}$ n/cm^2), the electrical and thermal conductivity of graphite increases due to radiation annealing. At high doses of radiation, the accumulation of radiation defects, vacancies and their small complexes occurs, due to this the electrical and thermal conductivity of graphite decreases. Fluence $>10^{22}$ n/cm^2 is the critical fluence of neutrons, which begins to graphite swelling, thermal conductivity decreases tens of times.

Conflict of interest statement

The authors declare that they have no conflict of interest in relation to this research, whether financial, personal, authorship or otherwise, that could affect the research and its results presented in this paper.

Credit author statement

Baytelesov S.A.: Writing - Original Draft; Tojiboev D.D.: Development of Facility and Measurements; Sadikov I.I.: Review & Editing; Kungurov F.R.: Conceptualization, Data Curation; Alikulov Sh.A.: Methodology, Investigation.
The final manuscript was read and approved by all authors.

References

1 Zhao Lu, Tang Jiang, Zhou Min, Shen Ke. (2022) A review of the coefficient of thermal expansion and thermal conductivity of graphite. *New Carbon Mater*, 37(3), 544–555. DOI: 10.1016/S1872-5805(22)60603-6.

2 Virgiliev Yu.S., Kalyagina I.P., Zemlyanikin V.F., Klimenko A.A. (2007) Graphite for the high-temperature gas-cooled reactor GT-MGR. *Atomic Energy*, 103 (4), 235 – 237. https://elib.biblioatom.ru/text/atomnaya-energiya_t103-4_2007/p235/ [in Russian].

3 Zhmurikov E.I., Romanenko A.I., Bulusheva L.G., Anikeeva O.B., Lavskaya Yu.V., Okotrub A.V., Abrosimov O.G., Tsybulya S.V., Logachev P.V., Tecchiol L. (2007) Studies of the electronic structure and properties of composites based on the ^{13}C carbon isotope. *Surface. X-ray, synchrotron and neutron studies*, 11, 29 – 35. https://elibrary.ru/item.asp?id=9554577&ysclid=lxvqu4h420350625560 [in Russian].

4 Zhmurikov E.I., Bolkhovityanov D.Yu., Blinov M.F., Ishchenko A.V., Kot N.Kh., Titov A.T., Tsybulya S.V., Tecchio L. (2010) On the issue of the durability of reactor graphites. *Surface. X-ray, synchrotron and neutron studies*, 5, 89 - 99. https://elibrary.ru/item.asp?id=15108600 [in Russian].

5 Zhang H., Lee G., Fonseca A.F., Bolders T.L., Cho K. (2010) Isotope effect on the thermal conductivity of graphene. *Journal of Nanomaterials*, Article ID 537657, 1 - 6. DOI: 10.48550/arXiv.1007.1496.

6 Belan E.P., Pokrovskiy A.S., Kharkov D.V. (2017) The effect of thermal annealing on thermal conductivity of graphite GR-280 irradiated up to high neutron fluence. *Physical and mathematical sciences*, I (1), 82 - 91. DOI:10.21685/2072-3040-2017-1-8. [in Russian].

7 Stankus S.V., Savchenko I.V., Agazhanov A.Sh., Yatsuk, O.S.; Zhmurikov, E.I. (2013) Thermophysical properties of MPG-6 graphite. *Thermophysics of High Temperatures*, 51(2), 205–209. https://www.mathnet.ru/php/archive.phtml?wshow =paper&jrnid=tvt&paperid=75&option_lang=eng [in Russian].

8 Vlasova K.P. (1964). *Graphite as a high-temperature material*. Collection of articles. 420. http://elcat.lib.misis.ru/vmsua5379ghkip/index.php?url=/notices/index/IdNotice:987677977/ Source:default# [in Russian].

9 Tadashi M., Masaaki H. (1992) Neutron irradiation effect on the thermal conductivity and dimensional change of graphite materials. *Journal of Nuclear Materials*, 195(1–2), 44-50. DOI: 10.1016/0022-3115(92) 90362-O.

10 Yumeng Zh., Yuhao J., Shasha L., Jie Gao., Zhou Zhou., Toyohiko Yano., Zhengcao Li. (2022) The Wigner energy and defects evolution of graphite in neutron-irradiation and annealing. *Radiation Physics and Chemistry*, 201, 110401. DOI: 10.1016/j.radphyschem.2022.110401.

11 Pavlov T.R., Lestak M., Wenman M.R., Vlahovic L., Robba D., Cambriani A., Staicu D., Dahms E., Ernstberger M., Brown M., Bradford M.R., Konings R.J.M., Grimes R.W. (2020) Examining the thermal properties of unirradiated nuclear grade graphite between 750 and 2500 K. *Journal of Nuclear Materials*, 538, 152176. DOI:10.1016/j.jnucmat.2020.152176.

12 Matthew S.L. Jordan., Paul R., Karen E. V., Tjark O. van Staveren., Matthew Brown., Bruce Davies., Nassia Tzelepi., Martin Metcalfe. (2018) Determining the electrical and thermal resistivities of radiolytically-oxidized nuclear

graphite by small sample characterization. *Journal of Nuclear Materials*, 507, 68 - 77. DOI:10.1016/j.jnucmat.2018.04.022.

13 Denisova E.I., Shaq A.V. (2005) *Measuring thermal conductivity using the IT-λ-400 meter*. Ekaterinburg, 35. https://study.urfu.ru/Aid/Publication/279/1/Denisova_Shak2.pdf [in Russian].

14 Abdukadyrova I.Kh., Alikulov Sh.A., Akhmedjanov F.R., Baytelesov S.A., Boltabaev A.F., Salikhbaev U.S. (2014) High-Temperature Thermal Conductivity of SAV-1 the Aluminum Alloys. *Atomic Energy*, 116 (2), 100 - 104. https://link.springer.com/content/pdf/10.1007/ s10512-014-9825-0.pdf

15 Instruction manual model 3207 digital micro-ohm meter. USA (2011), 35 https://www.instrumentation2000.com/pub/media/pdf/ballantine-3207-manual.pdf

16 Kuntse H.I. (1989) *Methods of physical measurements*. Moscow, 216. https://lib-bkm.ru/12583 [in Russian].

17 Anne A.C., Yutai K., Snead M.A., Takizawa K. (2016) Property changes of G347A graphite due to neutron irradiation. *Carbon*, 109, 860 - 873. DOI:10.1016/j.carbon.2016.08.042.

AUTHORS' INFORMATION

Baytelesov, Sapar Akimovich – Doctor (Sci.), Professor, Head of laboratory, Institute of Nuclear Physics, Uzbekistan Academy of Sciences, Ulugbek, Tashkent, Uzbekistan; SCOPUS Author iD: 9740002000; ORCID iD: 0000-0003-3926-9579; baytel@inp.uz

Tojiboev, Davronbek Davlatalievich – PhD student, Institute of Nuclear Physics, Academy of Sciences of Uzbekistan, Ulugbek, Tashkent, Uzbekistan; ORCID iD 0009-0006-0405-696X; tojiboyev_davron89@mail.ru

Sadikov, Ilkhom Ismailovich – Doctor (Sci.), Academician, Professor, Director, Institute of Nuclear Physics, Uzbekistan Academy of Sciences, Ulugbek, Tashkent, Uzbekistan; ORCID iD: 0000-0002-9779-370X, ilkham@inp.uz

Kungurov, Fakhrulla Rakhmatullayevich – Doctor (Sci.), Senior researcher, Deputy Director; Institute of Nuclear Physics, Uzbekistan Academy of Sciences, Ulugbek, Tashkent, Uzbekistan; ORCID iD: 0000-0003-4359-3523; fkungurov@inp.uz, +99871-2893758

Alikulov, Sherali Abdusalomovich – PhD, Senior researcher, Institute of Nuclear Physics, Uzbekistan Academy of Sciences, Ulugbek, Tashkent, Uzbekistan; ORCID iD: 0000-0003-4028-6501; alikulov@inp.uz; +99871-2893508